

and should be studied in detail.

In practice, as f_g is constant in the domain studied (for n_{OH} values ranged between 5 and 15 OH/nm²), the measure of f_g using only one ¹H DEC/MAS spectrum allows the determination of the concentration of hydroxyl groups in the sample. Therefore, we define a simple, routine experiment to characterize an amorphous silica.

The fact that the number of surface hydroxyl groups is greater than the theoretical value calculated on such surfaces implies that there is an internal surface only accessible to water molecules the size of which must be about the same as one of the external surface accessible to nitrogen or krypton molecules.

Registry No. Silica, 7631-86-9.

Solvent Effects on Electron Delocalization in Paramagnetic Organometallic Complexes: Solvent Manipulation of the Amount of 19-Electron Character in Co(CO)₃L₂ (L₂ = a Chelating Phosphine)

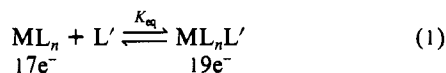
Fei Mao,¹ David R. Tyler,*¹ Mitchell R. M. Bruce,*² Alice E. Bruce,² Anne L. Rieger,³ and Philip H. Rieger*³

Contribution from the Departments of Chemistry, University of Oregon, Eugene, Oregon 97403, University of Maine, Orono, Maine 04469, and Brown University, Providence, Rhode Island 02912. Received February 19, 1992

Abstract: Infrared, ESR, and electronic absorption spectroscopic studies are reported on the 18+ δ Co(CO)₃L₂ complex. (L₂ is the chelating phosphine ligand 2,3-bis(diphenylphosphino)maleic anhydride. 18+ δ complexes are "19-electron complexes" in which the unpaired electron is primarily localized on a ligand.) The spectra are solvent dependent and are interpreted in terms of increased delocalization of the unpaired electron from an L₂(π^*) orbital onto the Co(CO)₃ portion of the molecule with decreasing solvent polarity. The relationship between the extent of delocalization onto the Co(CO)₃ and the substitution reactivity of the molecule was studied. Increased delocalization increases the rate of CO loss (and hence dissociatively activated substitution) because the acceptor molecular orbital on the Co(CO)₃ fragment is Co-CO antibonding ($k(\text{benzene}, 25^\circ) = (7.46 \pm 0.04) \times 10^{-2} \text{ s}^{-1}$; $k(\text{CH}_2\text{Cl}_2, 25^\circ) = (5.47 \pm 0.03) \times 10^{-3} \text{ s}^{-1}$). These substitution results are an exception to the rule of thumb which states that the lability of M-CO bonds decreases as the $\nu(\text{C}\equiv\text{O})$ frequencies decrease. An SCF-X α -SW calculation on the Co(CO)₃L₂' complex (L₂' = 2,3-bis(phosphino)maleic anhydride; i.e. L₂' is L₂ with the phenyl groups replaced by H atoms) confirmed previous ESR spectroscopic results which showed that the SOMO on the Co(CO)₃L₂ complex is primarily an L₂-based π^* orbital.

Introduction

Our laboratory is investigating the chemical, physical, and spectroscopic properties of 19-electron organometallic adducts.⁴⁻⁶ These complexes are formed by the reaction of 17-electron organometallic radicals with 2-electron-donor ligands:⁴⁻¹⁷



ML_n =

CpMo(CO)₃, CpW(CO)₃, CpFe(CO)₂, Mn(CO)₅, Co(CO)₄

L' = PR₃, P(OR)₃, NR₃, halides, pseudohalides, oxygen atom donors, CH₃CN, THF, and other coordinating solvents

The 19-electron adducts are reactive species, generally forming only as short-lived intermediates in radical reactions.^{5-7,18}

Our strategy for stabilizing the 19-electron complexes, so as to make them more amenable to study, is to introduce a ligand with a low-energy π^* orbital into the complex.^{4-6,10,19,20} Comparison of parts a and b of Figure 1 shows that if the ligand π^* orbital is sufficiently low in energy then the unpaired electron will

(10) Tyler, D. R.; Mao, F. *Coord. Chem. Rev.* **1990**, *97*, 119-140.

(11) (a) Fox, A.; Malito, J.; Poë, A. *J. Chem. Soc., Chem. Commun.* **1981**, 1052-1053. (b) Fawcett, J. P.; Jackson, R. A.; Poë, A. *J. Chem. Soc., Chem. Commun.* **1975**, 733-734.

(12) (a) Shi, Q.; Richmond, T. G.; Trogler, W. C.; Basolo, F. *J. Am. Chem. Soc.* **1982**, *104*, 4032-4034. (b) Trogler, W. C. *Int. J. Chem. Kinet.* **1987**, *19*, 1025-1047.

(13) Hershberger, J. W.; Klinger, R. J.; Kochi, J. *J. Am. Chem. Soc.* **1983**, *105*, 61-73.

(14) (a) Kidd, D. R.; Cheng, C. P.; Brown, T. L. *J. Am. Chem. Soc.* **1978**, *100*, 4103-4107. (b) McCullen, S. B.; Brown, T. L. *J. Am. Chem. Soc.* **1982**, *104*, 7496-7500. (c) Walker, H. W.; Rottinger, G. B.; Belford, R. L.; Brown, T. L. *Organometallics* **1983**, *2*, 775-776.

(15) It is interesting to note that K_{eq} has been measured for several of the reactions in which 19-electron adducts form. The formation of the 19-electron adduct is frequently thermodynamically downhill. See: Philbin, C. E.; Granatir, C. A.; Tyler, D. R. *Inorg. Chem.* **1986**, *25*, 4806. See also refs 16 and 17.

(16) Trogler, W. C.; Therien, M. J. *J. Am. Chem. Soc.* **1987**, *109*, 5127-5133.

(17) Kuchynka, D. J.; Kochi, J. K. *Inorg. Chem.* **1988**, *27*, 2574-2581.

(18) Typically, the reactivity of 19-electron complexes consists of either electron transfer to form a stable 18-electron complex or loss of a ligand to form a 17-electron species.⁵⁻⁷

(19) Mao, F.; Tyler, D. R.; Keszler, D. *J. Am. Chem. Soc.* **1989**, *111*, 130-134.

(20) Mao, F. Ph.D. Thesis, University of Oregon, 1990.

(1) University of Oregon.

(2) University of Maine.

(3) Brown University.

(4) Tyler, D. R. In *Organometallic Radical Processes*; Trogler, W. C., Ed.; Elsevier: New York, 1990; pp 338-364.

(5) Stiegman, A. E.; Tyler, D. R. *Comments Inorg. Chem.* **1986**, *5*, 215-245.

(6) Mao, F.; Philbin, C. E.; Weakley, T. J. R.; Tyler, D. R. *Organometallics* **1990**, *9*, 1510-1516.

(7) The adducts that form in the reactions of 17-electron species with ligands are known in the literature as "19-electron adducts" (or "19-electron complexes") simply because the sum of 17 valence electrons from the metal radical and 2 electrons from the ligand is 19. No implication about the electronic or geometric structures of these complexes is necessarily implied by this name. "Slipped" Cp rings, bent CO ligands (i.e., CO acting as a 1-electron donor), and phosphoranyl radical-type structures are all possible and would result in an 18- or 17-electron configuration at the metal center.

(8) Goldman, A. S.; Tyler, D. R. *Inorg. Chem.* **1987**, *26*, 253-258.

(9) Stiegman, A. E.; Tyler, D. R. *Coord. Chem. Rev.* **1985**, *63*, 217-240.

Table I. Selected SCF-X α -SW Molecular Orbitals for the Co(CO) $_3$ L $_2$ ' Complex^a

orbital	energy (eV)	% contribn														Co angular contribn
		Co	C(a)	C(b)	O(a)	O(b)	P	H(a)	H(b)	C(c)	C(d)	O(c)	O(d)	int	out	
23a''	-1.681	2	2	2	0	0	11	0	0	0	0	1	0	65	17	
31a'	-2.405	2	2	1	1	1	13	1	0	1	0	2	1	56	20	
30a'	-2.483	1	0	2	0	0	3	0	0	1	0	0	0	78	14	
22a''	-2.650	0	3	53	1	16	2	0	0	0	0	0	0	24	0	
21a''	-3.028	6	39	6	17	2	1	0	0	0	0	0	0	29	0	
29a'	-3.036	5	41	3	17	1	2	0	0	0	0	0	0	30	0	
20a''	-3.251	7	1	48	0	18	0	0	0	0	0	0	0	25	0	
28a'	-3.671	19	3	33	1	15	3	0	0	0	0	0	0	27	0	100% d
27a'	-3.881	12	0	42	0	19	1	0	0	0	0	0	0	25	0	100% d
19a''	-4.126	44	0	9	0	1	23	1	0	3	1	1	0	17	0	100% d
18a''	-4.184	2	0	1	0	0	5	1	1	33	14	16	0	27	0	
26a'	-7.000	57	6	5	1	5	6	0	1	0	0	0	0	19	0	1% s, 9% p, 90% d
17a''	-8.059	0	0	0	0	0	1	0	0	4	1	68	8	17	0	
25a'	-8.212	15	0	1	1	0	4	0	2	34	0	19	1	23	0	5% p, 95% d
16a''	-8.248	61	1	3	3	2	12	2	0	0	0	0	0	14	0	6% p, 94% d
24a'	-8.288	14	0	1	1	0	4	2	0	17	1	38	3	20	0	7% p, 93% d
23a'	-8.429	38	1	2	2	1	4	1	0	5	0	29	2	15	0	4% p, 96% d
22a'	-8.922	81	0	2	0	5	1	0	0	1	0	0	0	9	0	100% d
15a''	-9.700	50	0	2	0	2	28	2	4	0	0	0	0	11	0	6% p, 94% d
21a'	-9.995	0	0	0	0	0	1	0	1	7	5	32	36	18	0	

^aThe 18a'' and 19a'' orbitals are the SOMO and LUMO, respectively.

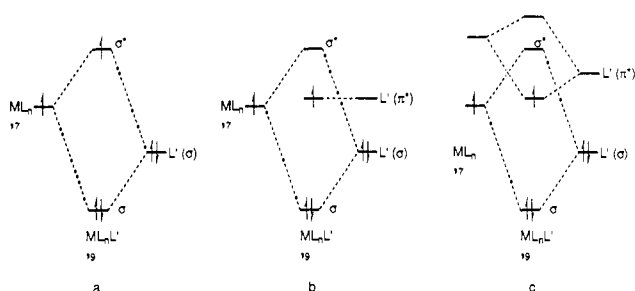


Figure 1. (a) Simplified molecular orbital scheme showing the interaction of the singly occupied orbital on a 17-electron organometallic radical with a ligand orbital to form a 19-electron complex. Note that the unpaired ("19th") electron occupies a M-L antibonding orbital. (b) Same as (a) except that the ligand has a low-energy π^* orbital. This scheme is applicable to "18+ δ " complexes. The unpaired electron now occupies the π^* orbital. (c) Same as (b) except that an additional orbital on the metal is shown interacting with the ligand π^* orbital. This latter interaction leads to delocalization of the unpaired electron onto the metal.

preferentially occupy the ligand π^* orbital, rather than a M-L σ^* orbital, with a concomitant increase in stability of the complex. Nineteen-electron complexes of this type have been dubbed "18+ δ " complexes⁶ because they can be described as 18-electron complexes with partial electron density contributed to the metal by delocalization of the unpaired electron from the reduced ligand (Figure 1c).²¹

(21) Despite the increased stability compared to the stability of the photogenerated 19-electron complexes, it should be noted that the 18+ δ complexes can still be quite reactive and difficult to isolate and characterize.^{22,23}

(22) Examples of 18+ δ complexes are increasingly numerous. See: (a) Kaim, W. *Coord. Chem. Rev.* **1987**, *76*, 187-230. (b) Creber, K. A. M.; Wan, J. K. S. *Transition Met. Chem. (London)* **1983**, *8*, 253-254. (c) Creber, K. A. M.; Wan, J. K. S. *J. Am. Chem. Soc.* **1981**, *103*, 2101-2102. (d) Alberti, A.; Hudson, A. *J. Organomet. Chem.* **1983**, *241*, 313-319. (e) Kaim, W. *Coord. Chem. Rev.* **1987**, *76*, 187. (f) Kaim, W.; Kohlmann, S. *Inorg. Chem.* **1986**, *25*, 3442-3448. (g) Kaim, W. *J. Organomet. Chem.* **1984**, *262*, 171-178. (h) Kaim, W. *Inorg. Chim. Acta* **1981**, *53*, L151-L153. (i) Kaim, W. *Inorg. Chem.* **1984**, *23*, 3365-3368. (j) Alegria, A. E.; Lozada, O.; Rivera, H.; Sanchez, J. *J. Organomet. Chem.* **1985**, *281*, 229-236. (k) Andrea, R. R.; de Lange, W. G. J.; van der Graff, T.; Rijkhoff, M.; Stufkens, D. J.; Oskam, A. *Organometallics* **1988**, *7*, 1100-1106 and references therein. (l) Kokkes, M. W.; de Lange, W. G. J.; Stufkens, D. J.; Oskam, A. *J. Organomet. Chem.* **1985**, *294*, 59. (m) Franz, K.; tom Dieck, H.; Krynitz, U.; Renk, I. *W. J. Organomet. Chem.* **1974**, *64*, 361-366. (n) Franz, K.; tom Dieck, H.; Starzewski, K.; Hohmann, F. *Tetrahedron* **1975**, *31*, 1465-1549. (o) Alberti, A.; Hudson, A. *J. Organomet. Chem.* **1983**, *248*, 199-204. (p) Maroney, M. J.; Trogler, W. C. *J. Am. Chem. Soc.* **1984**, *106*, 4144-4151. (q) Kaim, W.; Gross, R. *Comments Inorg. Chem.* **1988**, *7*, 269-285. (r) Kaim, W.; Olbrich-Deussner, B. In *Organometallic Radical Processes*; Trogler, W. C., Ed.; Elsevier: New York, 1990; pp 173-200. (s) Gross, R.; Kaim, W. *Inorg. Chem.* **1986**, *25*, 498-506. (t) Kaim, W. *Inorg. Chem.* **1984**, *23*, 504-505.

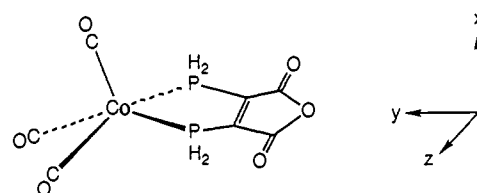
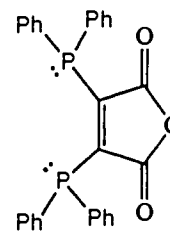


Figure 2. Coordinate system used for the SCF-X α -SW calculation on Co(CO) $_3$ L $_2$ '.

In order to learn more about the 18+ δ complexes and their relationship to "genuine" 19-electron complexes, we are investigating three aspects of their chemistry: (1) How are the relative amounts of "19-electron character" in a series of 18+ δ complexes determined? (The "amount of 19-electron character" is defined in this paper in a relative sense: in the comparison of two 18+ δ complexes, the one in which the unpaired electron is more delocalized onto the metal is said to have more 19-electron character.) (2) Can we manipulate the amount of 19-electron character in an 18+ δ complex? (3) Is there a correlation between the reactivity and the amount of 19-electron character in an 18+ δ complex?

In this paper we answer these questions for the Co(CO) $_3$ L $_2$ complex (L $_2$ is the chelating phosphine ligand 2,3-bis(diphenylphosphino)maleic anhydride).²³ We demonstrate that the amount



2,3-bis(diphenylphosphino)maleic anhydride (L $_2$)

of "19-electron character" is sensitive to the solvent, and we show how the extent of electron delocalization affects the substitution reactivity of the molecule. To assist in the interpretation of our experimental results, an SCF-X α -SW calculation was done on the complex, and we also report the results of the calculation herein.

(23) Fenske, D. *Chem. Ber.* **1979**, *112*, 363-375.

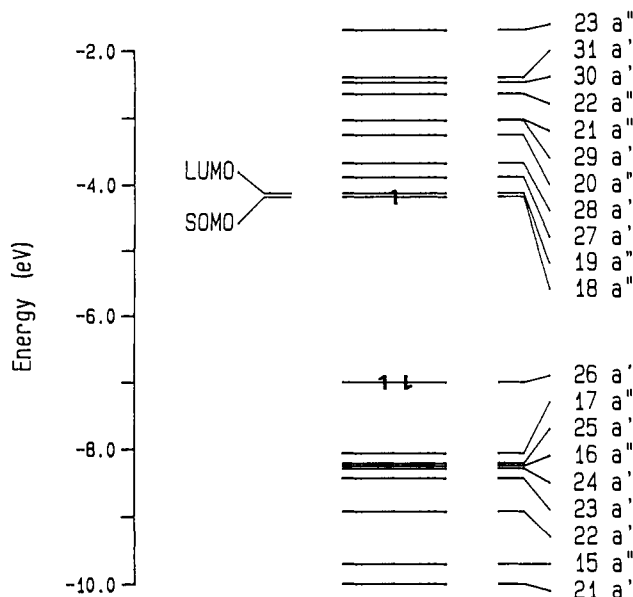


Figure 3. Ground-state eigenvalues and primary orbital character for $\text{Co}(\text{CO})_3\text{L}_2'$.

Results and Discussion

Delocalization of the Unpaired Electron in $18+\delta$ Complexes: SCF- $X\alpha$ -SW Calculation on the $\text{Co}(\text{CO})_3\text{L}_2'$ Complexes. The MO scheme in Figure 1b is incomplete in the sense that it does not show the delocalization of the unpaired electron onto the metal.

Table II. IR Data for the $\text{Co}(\text{CO})_3\text{L}_2$ Complex in Various Solvents

solvent	E_T^N ^a	$\bar{\nu}(\text{C}\equiv\text{O})$ (cm^{-1})	$\bar{\nu}(\text{C}=\text{O})$ (cm^{-1})
toluene	0.099	2076, 2026, 2002	1748, 1691
benzene	0.111	2076, 2027, 2003	1747, 1679
<i>p</i> -dioxane	0.164	2076, 2026, 2003	1747, 1678
THF	0.207	2077, 2027, 2006	1747, 1679
<i>o</i> -dichlorobenzene	0.225	2078, 2029, 2009	1744, 1674
DME	0.231	2077, 2027, 2006	1747, 1678
dichloromethane	0.309	2080, 2031, 2009	1742, 1670
1,2-dichloroethane	0.327	2080, 2031, 2010	1743, 1671
acetone	0.355	2081, 2030, 2011	..., ^b ..., ^b
aniline	0.420	2080, 2031, 2009	1738, 1667
acetonitrile	0.460	2082, 2030, 2013	1742, 1672
propylene carbonate	0.491	2082, 2031, 2013	..., ^b 1669

^a See ref 26 for a definition of the solvent polarity parameter E_T^N .

^b These bands could not be observed because of the strong absorbance of the solvent.

The delocalization is shown qualitatively in the enhanced scheme in Figure 1c. In order to learn more about the metal orbitals involved in the delocalization of the unpaired electron and in order to interpret better the spectroscopic properties of the $\text{Co}(\text{CO})_3\text{L}_2$ complex, we performed an SCF- $X\alpha$ -SW molecular orbital calculation on the complex. To simplify the calculation, the phenyl rings on the L_2 ligand were replaced by H atoms; this modified ligand is denoted by L_2' .

Figure 2 shows the coordinate system used for the calculation, the results of which are summarized in Table I and Figure 3. The singly occupied molecular orbital (SOMO; the $18a''$ orbital) is primarily the lowest energy π^* orbital on the L_2' ligand, consistent with earlier ESR conclusions.^{19,23,24} A plot of the SOMO is shown

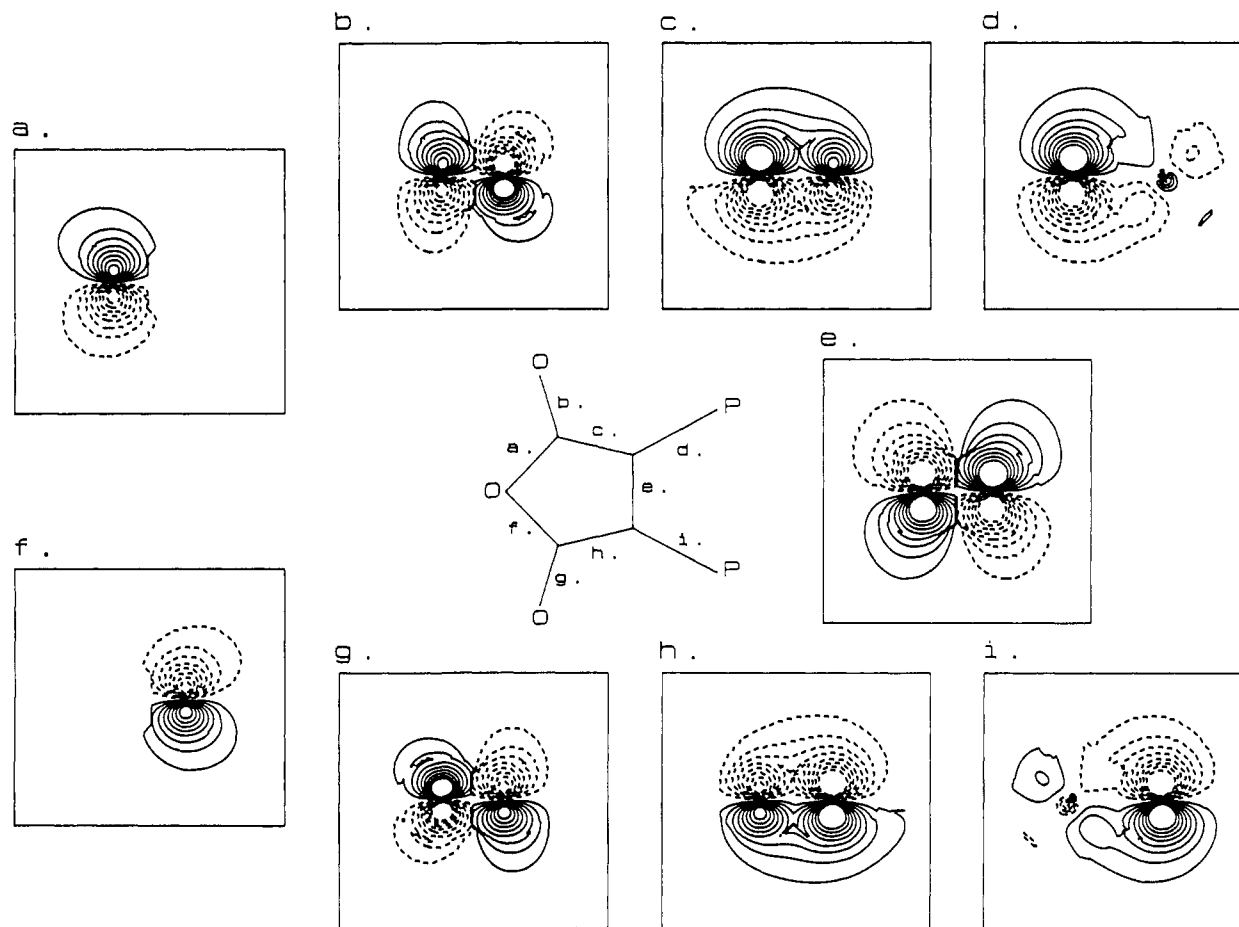


Figure 4. Wave-function contour plots for the SOMO in the $\text{Co}(\text{CO})_3\text{L}_2$ complex. The orbital is delocalized over the ring, and the letter of each plot corresponds to the section of the ring indicated by the same letter; i.e. plot b corresponds to the bond labeled b (a $\text{C}=\text{O}$ bond). The bond is plotted as if the eye were located where the letter is located. Thus, in plot b the carbon atom is on the left side of the plot and the oxygen is on the right. Wave-function density is plotted in the plane containing the bond perpendicular to the plane of the maleic anhydride ring. Solid and broken lines denote contours of opposite sign at values of ± 0.010 , ± 0.020 , ± 0.030 , ± 0.040 , ± 0.050 , ± 0.060 , ± 0.070 , and ± 0.080 electron^{1/2} bohr^{-3/2}.

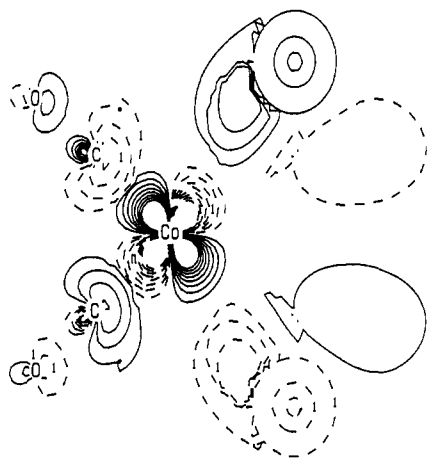


Figure 5. Wave-function contour plot for the SOMO in the plane containing the Co and C(O) atoms. The Co-C bonds are on the left-hand side of the plot; note that the interaction is antibonding.

in Figure 4. The SOMO also has a small amount of Co-CO_{eq} antibonding character, as shown in Figure 5. This antibonding character is likely responsible for the lability of the Co-CO bond in the complex, as discussed further below.¹⁹ The LUMO orbital (19a'') is primarily Co in character with substantial contribution from phosphorus. Orbital plots show that this orbital is the antibonding counterpart of the 15a'' Co-P bonding orbital.

The SOMO and LUMO orbitals are very close in energy, as well as close in energy to a series of CO(π^*) orbitals (27a', 28a', etc.). In fact, the accuracy of the calculation is such that it cannot be used to distinguish the various energy orderings of the 18a'', 19a'', 27a', and 28a' orbitals.²⁵ Nevertheless, we are confident that the SOMO orbital is indeed the L₂(π^*) orbital, as predicted by the calculation, because our previous ESR study²⁴ showed that the Co 3d unpaired spin density is only 0.016. If 19a'' were the SOMO, we would see a much larger unpaired spin density on Co. Similarly, if a CO(π^*) orbital were the SOMO, then we would not see strong coupling to the P atoms ($a_P = 9.72$ G in CH₂Cl₂), but coupling to the CO carbon atoms would be large. As we showed in a previous paper,¹⁹ the coupling to ¹³C in the Co(¹³C-O)₃L₂ complex is quite small. Finally, one other fact suggests that the SOMO is the L₂(π^*) orbital: H atoms were used in place of phenyl groups on the P atoms for the calculation. The electron-withdrawing ability of the phenyl rings will stabilize the L₂(π^*) orbital in Co(CO)₃L₂ and therefore lower its energy relative to the LUMO and CO(π^*) orbitals.

In summary, the X α calculation reinforces the experimental results^{19,23} which showed that the unpaired electron is primarily localized on the L₂ ligand. Orbital plots (Figure 5) show that the SOMO also has a small Co-CO antibonding component.

Relative Amounts of "19-Electron Character" in the 18+ δ Complexes: Infrared Spectroscopy. The frequencies of the C \equiv O and C=O stretching bands in the Co(CO)₃L₂ complex are solvent sensitive. Infrared data acquired in 12 different solvents are found in Table II and plotted as a function of solvent polarity in Figure 6. (The Reichardt E_T^N scale was used as a measure of solvent polarity in Figure 6.²⁶) Note that the frequencies of the three C \equiv O bands decrease with decreasing solvent polarity and the two C=O bands increase in frequency. We attribute the solvent-dependent frequencies to increased delocalization of the unpaired electron from the L₂(π^*) orbital onto the Co(CO)₃ moiety in nonpolar solvents compared to polar solvents; i.e., the Co(CO)₃L₂ complex has more 19-electron character in nonpolar

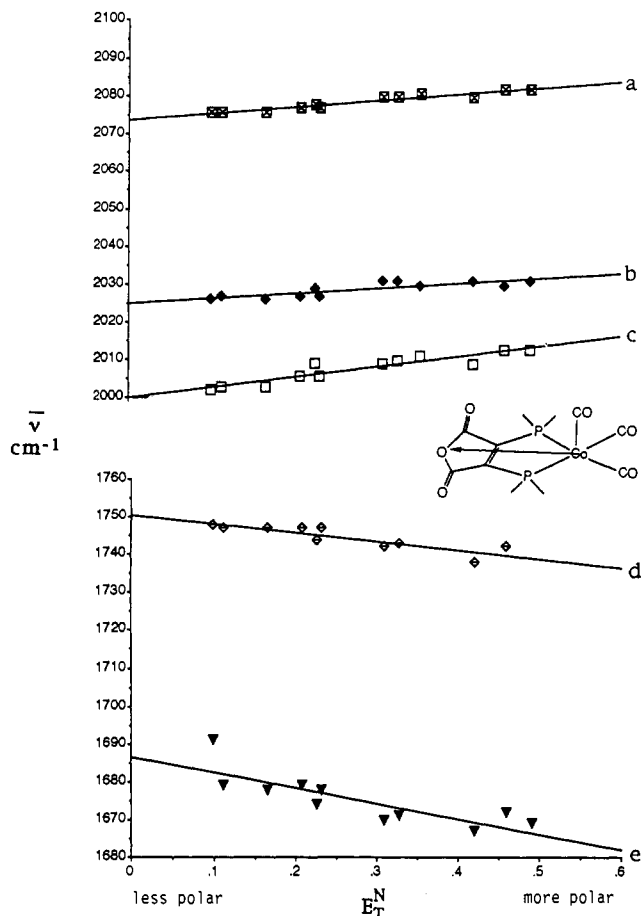


Figure 6. Plot of $\nu(\text{CO})$ (cm⁻¹) in various solvents (296 K) vs the Reichardt E_T^N parameters for those solvents. The lines labeled a-c refer to the three C \equiv O bands, and the d and e lines are the C=O bands. Insert: The dipole direction (in the yz plane) for the Co(CO)₃L₂ complex.

solvents than in polar solvents. This result is explained as follows. In polar solvents, it is energetically favorable for the electron to remain localized on the L₂ ligand because localization gives the largest molecular dipole (see the insert in Figure 6) and hence the largest dipolar interactions with the solvent. In less polar solvents, however, dipolar interactions with the solvent are energetically less important,²⁷ and a lower energy state is obtained by delocalizing the electron onto the Co(CO)₃ moiety from the L₂(π^*) orbital. The $\nu(\text{C}=\text{O})$ bands increase in frequency with increasing delocalization because the lowest energy π^* orbital on L₂ is C=O antibonding (Figure 4) and it is being depopulated. The C \equiv O bands decrease in frequency with increasing delocalization onto the Co(CO)₃ moiety due to increased π -back-bonding.²⁸

In summary, these results show that one way to manipulate the amount of 19-electron character in an 18+ δ complex is to change the solvent. Furthermore, infrared spectroscopy (as well as ESR and electronic absorption spectroscopy; see below) can be used to determine the relative amounts of 19-electron character in 18+ δ complexes.

It is important to note that the solvent shifts depicted in Figure 6 are in the direction opposite to the normal solvent shifts observed with metal carbonyl complexes.²⁹ That is, for most metal carbonyl complexes, an increase in solvent polarity leads to a decrease in

(24) Mao, F.; Tyler, D. R.; Rieger, A. L.; Rieger, P. H. *J. Chem. Soc., Faraday Trans.*, in press.

(25) Bruce, M. R. M.; Kenter, A.; Tyler, D. R. *J. Am. Chem. Soc.* **1984**, *106*, 639.

(26) (a) Reichardt, C. *Angew. Chem., Int. Ed. Engl.* **1965**, *4*, 29. (b) In this paper, we use the dimensionless, normalized parameter E_T^N . See: Reichardt, C. *Solvents and Solvent Effects in Organic Chemistry*, 2nd ed.; VCH Publishers: New York, 1988; p 364.

(27) Gross, R.; Kaim, W. *J. Organomet. Chem.* **1987**, *333*, 347-365.

(28) The Co/CO interaction in the SOMO has little, if any π -bonding character. Therefore, the increased π -back-bonding cannot be directly attributed to the increased Co/CO character of the SOMO. However, the increased electron density on Co will increase the π -back-bonding of the other Co d orbitals, and this will lead to the decreased C=O frequencies.

(29) Solvent effects on C=O stretching frequencies are reviewed in: Haines, L. M.; Stiddard, M. H. B. *Adv. Inorg. Chem. Radiochem.* **1969**, *12*, 53-133 (see p 100).

Table III. Coupling Constants (G) for $\text{Co}(\text{CO})_3\text{L}_2$ in Various Solvents^a

solvent	$a^{\text{P}}(250 \text{ K})$	$a^{\text{P}}(300 \text{ K})$	$a^{\text{Co}}(250 \text{ K})$	$a^{\text{Co}}(300 \text{ K})$
toluene	11.43	11.06	1.47	1.51
benzene		11.13		1.47
diethyl ether	11.47	11.23	1.36	1.45
THF	11.27	11.05	1.24	1.30
dichloromethane	11.20	10.99	1.19	1.20
1,2-dichloroethane	11.25	11.04	1.25	1.20
acetone	11.18	10.98	1.23	1.19
acetonitrile	11.11	10.88	1.31	1.19

^a $g = 2.0042 \pm 0.0002$.**Table IV.** Band Maximum of the Lowest Energy Transition in the Electronic Absorption Spectrum of the $\text{Co}(\text{CO})_3\text{L}_2$ Complex in Various Solvents (296 K)

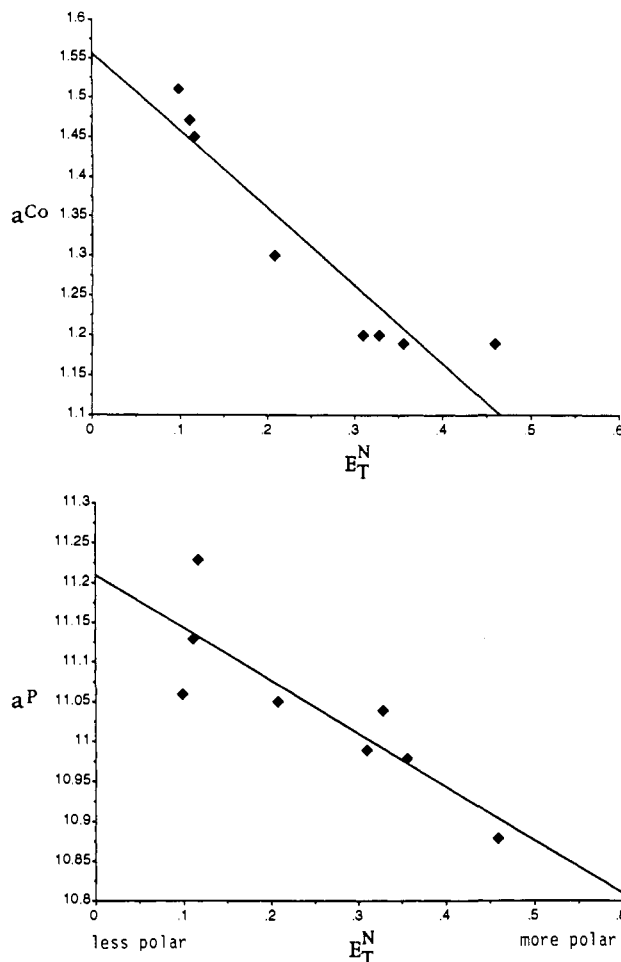
solvent	ϵ^a	$E_{\text{T}}^{\text{N}b}$	λ (nm)	$\bar{\nu}$ (cm^{-1})
toluene	2.438	0.099	840	11 900
benzene	2.284	0.111	835	12 000
diethyl ether	4.335	0.117	836	12 000
<i>p</i> -dioxane	2.209	0.164	825	12 100
THF	7.580	0.207	806	12 400
<i>o</i> -dichlorobenzene	9.93	0.225	782	12 800
DME		0.231	792	12 600
dichloromethane	9.08	0.309	758	13 200
1,2-dichloroethane		0.327	757	13 200
acetone	20.70	0.355	754	13 300
aniline	6.89	0.420	714	14 000
acetonitrile	37.5	0.460	716	14 000
propylene carbonate	65.1	0.491	730	13 700

^a Dielectric constant. ^b See ref 26 for a definition of the solvent polarity parameter E_{T}^{N} .

the frequencies of the C=O stretching bands. There is no reason to believe that the $\text{Co}(\text{CO})_3\text{L}_2$ complex is an exception to this rule, say, because of the L_2 ligand. For example, the $\nu(\text{C}=\text{O})$ frequency shifts in the related (18-electron) $\text{Cr}(\text{CO})_4\text{L}_2$ complex are in the normal direction; i.e., increasing polarity shifts the bands to lower frequency ($\nu(\text{C}=\text{O})$ (cm^{-1}): 2021 (m), 1937 (m), and 1910 (s) in CCl_4 ; 2019 (m), 1928 (m), 1909 (s), and 1897 (s) in CH_3CN).³⁰ The point here is that the solvent shifts depicted in Figure 6 are not just the normal shifts observed for metal carbonyl complexes. The peak shifts have a different origin, namely, we propose, solvent-induced changes in the amount of 19-electron character in the complex.

ESR Spectra. The ESR spectra are also consistent with increased delocalization of the unpaired electron in nonpolar solvents. The spectral data in various solvents are summarized in Table III, and the coupling constants are plotted vs solvent polarity in Figure 7. Note the overall trend: the P and Co coupling constants generally increase as the polarity of the solvent decreases. An increase in the cobalt coupling constant reflects a larger cobalt 3d spin density, which in turn is indicative of increased delocalization from the ligand onto the metal. Because of possible spin-polarization effects which may lead to negative contributions to the coupling constant, the phosphorus coupling is more difficult to interpret. However, since the phosphorus coupling is substantially larger in $\text{Co}(\text{CO})_3\text{L}_2$ than in the L_2 radical anion,²⁴ it is likely that the phosphorus coupling can be taken as a measure of spin density on the phosphorus atoms. Thus an increase in phosphorus coupling is also indicative of increased delocalization.

Electronic Spectra. Finally, the electronic spectrum of the $\text{Co}(\text{CO})_3\text{L}_2$ complex is also consistent with the increased delocalization of the unpaired electron in nonpolar solvents. The electronic spectrum exhibits a single, broad absorption band in the visible/near-IR region (Table IV). The peak maximum of this band is solvent dependent, shifting, for example, from 714 nm ($14\,000 \text{ cm}^{-1}$) in aniline to 840 nm ($11\,900 \text{ cm}^{-1}$) in toluene (Table IV). Electrochemical oxidation of the complex to $\text{Co}(\text{CO})_3\text{L}_2^+$ causes the low-energy band to disappear. Because the unpaired electron in the $\text{Co}(\text{CO})_3\text{L}_2$ complex is primarily localized on the chelate ligand, the disappearance of the absorption band

**Figure 7.** ESR coupling constants (300 K) for the $\text{Co}(\text{CO})_3\text{L}_2$ complex in various solvents plotted as a function of the Reichardt E_{T}^{N} parameters for those solvents.

in the oxidized complex suggests that the band may be attributable to an internal transition in the reduced ligand, L_2^- . However, the electronic spectrum of the L_2^- species (formed electrochemically by reduction of L_2) shows no bands in the near-IR/visible region. Thus, the band for $\text{Co}(\text{CO})_3\text{L}_2$ cannot be attributed to a $\pi^* \rightarrow \pi^*$, $n \rightarrow \pi^*$, or some other ligand-centered transition.³¹

Inspection of the simple MO scheme in Figure 1b or 1c suggests that the electronic absorption band be assigned to a $\text{L}_2(\pi^*) \rightarrow \sigma^*$ transition, i.e. a ligand-to-metal charge-transfer transition.³³ This assignment is consistent with the observed solvatochromism because the excitation decreases the magnitude of the molecular dipole moment (insert, Figure 6). In such cases, it is well established³⁴ that the LMCT transition will blue-shift with increasing solvent polarity. Because the size of the ground-state dipole is inversely related to the extent of delocalization, the shift in the band maximum is an indicator of the amount of odd-electron delocalization in the complex.

As was the case with the infrared and ESR data, the energy of the $\text{Co}(\text{CO})_3\text{L}_2$ absorption band in the various solvents is linear when plotted vs the E_{T}^{N} scale (Figure 8).^{35,37,39}

(31) Note that d-d transitions are, in general, insensitive to the change of solvent polarity.³²(32) Lever, A. B. P. *Inorganic Electronic Spectroscopy*, 2nd ed.; Elsevier: Amsterdam, 1984.(33) The SCF-X α -SW calculation also suggests this assignment. However, in the absence of a transition-state calculation, we are reluctant to cite the calculation as supporting evidence for such an assignment.(34) (a) See ref 32, p 208 ff. (b) Olbrich-Deussner, B.; Kaim, W.; Gross-Lannert, R. *Inorg. Chem.* 1989, 28, 3113-3120.(35) Burgess et al.³⁶ have shown that the energy of charge-transfer transitions is often linearly proportional to the empirical Reichardt E_{T}^{N} parameter.(36) Burgess, J.; Chambers, J. G.; Haines, R. I. *Transition Met. Chem. (London)* 1981, 6, 145.

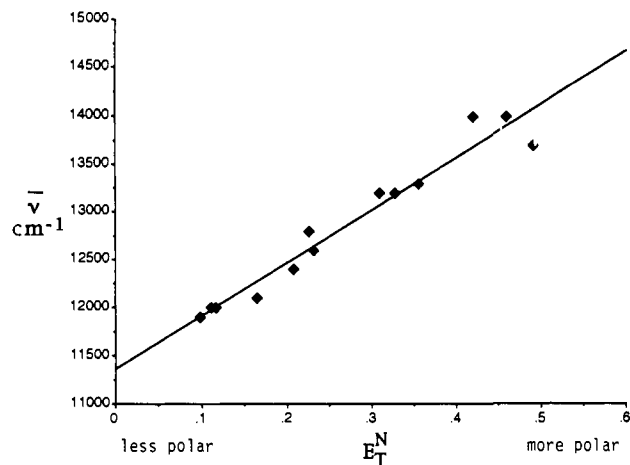


Figure 8. Plot of the electronic absorption band maximum (296 K) in various solvents vs the Reichardt E_T^N parameters for those solvents.

Table V. Rate Constants and Activation Parameters for the Substitution of $\text{Co}(\text{CO})_3\text{L}_2$ by PPh_3 in Benzene and CH_2Cl_2

	CH_2Cl_2	C_6H_6
$k(25^\circ\text{C}) (\text{s}^{-1})^a$	$(5.47 \pm 0.03) \times 10^{-3}$	$(7.46 \pm 0.04) \times 10^{-2}$
ΔH^\ddagger (kcal/mol)	23.8 ± 0.6	19.83 ± 0.54
ΔS^\ddagger (cal/(mol K))	11.1 ± 2.2	2.82 ± 1.87

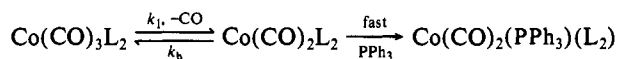
^a k is independent of the ligand concentration.

In summary, the results above show that it is possible to determine the relative amounts of 19-electron character in an $18+\delta$ complex by using infrared, ESR, and electronic absorption spectroscopy. In addition, the results show that one way to manipulate the amount of 19-electron character in an $18+\delta$ complex is to change the polarity of the solvent.

Relationship between the Amount of 19-Electron Character and the Rate of Substitution. The spectroscopic interpretations presented in the sections above suggest that the $\text{Co}(\text{CO})_3\text{L}_2$ complex will be more labile in nonpolar solvents than in polar solvents. The reason is straightforward: the unpaired electron is more delocalized from the L_2 ligand onto the $\text{Co}(\text{CO})_3$ moiety in nonpolar solvents; as shown by the $X\alpha$ calculation, the $\text{Co}(\text{CO})_3$ acceptor orbital is $\text{Co}-\text{CO}$ antibonding (Figures 1c and 5), and thus increased delocalization will weaken the $\text{Co}-\text{CO}$ bond.

The prediction of increased lability in nonpolar solvents was confirmed by experiment. In a previous study, we showed¹⁹ that $\text{Co}(\text{CO})_3\text{L}_2$ substitutes via a limiting dissociative mechanism in CH_2Cl_2 (Scheme I). The rate constant for CO loss was $(5.47 \pm 0.03) \times 10^{-3} \text{ s}^{-1}$ (k_1 in Scheme I). For comparison, we repeated the measurement of k_1 in benzene in the present study and found $k = (7.46 \pm 0.04) \times 10^{-2} \text{ s}^{-1}$, a value almost 14 times larger than that in CH_2Cl_2 . The activation parameters (Table V) and the fact that the rate is independent of ligand concentration suggest that the same dissociative reaction mechanism applies in benzene as in CH_2Cl_2 , and therefore the rate constant in benzene compared to CH_2Cl_2 reflects an increased rate of CO loss.

Scheme I



(37) Studies by tom Dieck et al.^{34a,38} showed that $\nu(\text{C}\equiv\text{O})$ in complexes containing an $\text{ML}_2(\text{CO})_2$ plane ($\text{L}_2 =$ a conjugated chelating ligand) often showed solvent effects and that only the in-plane CO stretching bands showed a solvent effect; bands attributed to carbonyls in the axial position were little affected. The $\text{CoL}_2(\text{CO})_2$ unit is not planar in $\text{Co}(\text{CO})_3\text{L}_2$, so a similar criterion cannot be used to assign the bands.

(38) tom Dieck, H.; Renk, I. W. *Angew. Chem., Int. Ed. Engl.* 1970, 9, 793.

(39) Similar to tom Dieck's results,^{34a,38} a linear relationship was also obtained between the energy of the optical charge-transfer transition and the $\text{C}-\text{O}$ stretching frequencies. This plot, which is similar in appearance to Figure 6, is provided as supplementary material.

It is interesting to note that the results of this substitution experiment are an exception to the rule of thumb which states that the lability of $\text{M}-\text{CO}$ bonds decreases as the $\nu(\text{C}\equiv\text{O})$ frequencies decrease.⁴⁰ The rationale for this rule comes from the fact that lower $\text{C}\equiv\text{O}$ stretching frequencies are indicative of increased π -back-bonding, i.e., stronger $\text{M}-\text{CO}$ bonding. In the $\text{Co}(\text{CO})_3\text{L}_2$ complex, as unpaired electron density is delocalized from the L_2 ligand onto the $\text{Co}(\text{CO})_3$ fragment, π -back-bonding does indeed increase, as reflected in the lower $\text{C}\equiv\text{O}$ stretching frequencies.²⁸ However, the increase in the $\text{Co}-\text{CO}$ π bonding is more than offset by the decrease in the σ bonding, caused by electronic occupation of a $\text{Co}-\text{C}$ antibonding orbital (Figures 1c and 5). The complex is thus more labile in nonpolar solvents despite the increase in π -back-bonding.

Conclusions. The spectroscopic properties and substitution reactivity of the $\text{Co}(\text{CO})_3\text{L}_2$ complex are dependent on the solvent polarity. The origin of the solvent-dependent properties lies in the variable extent of unpaired-electron delocalization: the unpaired electron is increasingly delocalized from the L_2 ligand onto the $\text{Co}(\text{CO})_3$ fragment in solvents of decreasing polarity. We hypothesize that, in addition to substitution, other types of reactivity can be controlled as well. We are currently investigating how the extent of delocalization affects CO insertion and electron-transfer reactions of $18+\delta$ complexes.

Experimental Section

Unless otherwise noted, all manipulations were done under an inert atmosphere using standard Schlenk techniques or a Vacuum Atmospheres Co. glovebox.

Materials and Supplies. Reagent grade solvents were dried and distilled using literature methods.⁴¹ Toluene, benzene, diethyl ether, *p*-dioxane, and DME were distilled over Na. THF was distilled over K. $\text{CH}_2\text{ClCH}_2\text{Cl}$, CH_2Cl_2 , CH_3CN , *o*-dichlorobenzene, and aniline were distilled over CaH_2 . Acetone was distilled over anhydrous K_2CO_3 . Propylene carbonate (Gold Label) was purchased from Aldrich and used as received. Acetonitrile (Aldrich Gold Label) for use in the electrochemical experiments was degassed and stored in the drybox under nitrogen. Cyclohexylamine and 40% aqueous glyoxal solution (Aldrich) were used as received. PPh_3 was purchased from Sigma and recrystallized from hexane. $\text{Co}(\text{CO})_3\text{L}_2$ and L_2 were synthesized as previously described.^{6,19} Cp_2Co and $[\text{Cp}_2\text{Co}]\text{PF}_6$ (Strem) were used as received. $[\text{NMe}_4]\text{PF}_6$ was recrystallized twice from ethanol/water, dried under vacuum for 15 h over P_2O_5 at 90° , and stored in the glovebox.

Instrumentation. Electronic absorption spectra were recorded on a Beckman DU spectrophotometer. Infrared spectra were recorded on a Nicolet 5DXB FT-IR instrument with CaF_2 cells (solution) or NaCl plates (Nujol mull). ^1H NMR spectra were obtained on a Varian XL 200 instrument. ESR spectra were recorded on a Bruker ER-220D spectrometer, which was equipped with an ASPECT-2000 computer, a Systron-Donner 6246A microwave frequency counter, a Bruker NMR gaussmeter, and a Bruker variable-temperature unit. Electrochemical experiments were performed as previously described.¹⁹ Ferrocene was used as an internal standard in the electrochemistry experiments. The redox potential of ferrocene in 0.1 M $(n\text{-Bu})_4\text{N}^+\text{PF}_6^-/\text{CH}_3\text{CN}$ in our system was 0.40 V vs SCE with a peak-to-peak separation of 80 mV. The bulk electrochemical reduction of L_2 was carried out in THF using a Princeton Applied Research Electrochemical Station. Infrared spectrum of $(n\text{-Bu})_4\text{N}^+\text{L}_2^-$ in THF: 1725 (s), 1635 (s) cm^{-1} . Kinetics experiments were carried out as previously described.¹⁹ The rates of $\text{Co}(\text{CO})_3\text{L}_2$ disappearance were independent of PPh_3 concentration.

Molecular Orbital Calculations of $\text{Co}(\text{CO})_3\text{L}_2^-$. The calculation was carried out by the SCF- $X\alpha$ -SW method⁴² using a DEC VAX 11/780

(40) An example is provided by the rate constants for dissociative substitution of the $\text{Mn}(\text{CO})_5\text{X}$ complexes ($\text{X} = \text{Cl}, \text{Br}, \text{I}$): $k = 2.6 \times 10^{-3}$, 3.3×10^{-4} , and $1.6 \times 10^{-5} \text{ s}^{-1}$, respectively, for substitution of the Cl, Br, and I complexes by AsPh_3 in CHCl_3 solvent. For further examples and further discussion of this point see: Basolo, F.; Pearson, R. G. *Mechanisms of Inorganic Reactions*; Wiley: New York, 1967; pp 561-571. Note that the rule of thumb assumes that only electronic factors are variable and that steric factors are held constant.

(41) Perrin, D. D.; Armarego, W. L. F.; Perrin, D. R. *Purification of Laboratory Chemicals*; Pergamon: Oxford, England, 1980.

(42) (a) Slater, J. C. *The Calculation of Molecular Orbitals*; Wiley: New York, 1979; see also references therein. (b) Johnson, K. H. *Adv. Quantum Chem.* 1973, 7, 143. (c) Rosch, N.; Klemperer, W. G.; Johnson, K. H. *Chem. Phys. Lett.* 1973, 23, 149. (d) Johnson, K. H.; Smith, F. C. *Phys. Rev. B.* 1972, 5, 831.

and Macintosh SE/30 computers.⁴³ Norman's procedure for interpolation of overlapping-sphere sizes was used to optimize the virial coefficient at 1.^{44,45} Schwarz's α_{HF} values⁴⁶ were used for the atomic exchange parameters, except for hydrogen, in which case Slater's value⁴⁷ of 0.7725 was used. The α values for the intersphere and outer-sphere regions were weighted averages of the atomic α values, where the weights are the number of valence electrons on the different neutral free atoms.

A minimal basis set in partial wave expansion was used for all calculations.⁴⁸ Using $l = 1$ for the outer-sphere region was sufficient to generate basis function components in all representations.

(43) (a) Convergence was obtained on a DEC VAX 11/780 computer using codes previously reported: Bruce, M. R. M.; Kenter, A.; Tyler, D. R. *J. Am. Chem. Soc.* **1984**, *106*, 640. (b) Wave-function contour plots were generated on a Macintosh SE/30 computer using a Language Systems Fortran compiler. Plots were made on a Hewlett Packard ColorPro plotter.

(44) (a) Norman, J. G., Jr. *J. Chem. Phys.* **1974**, *61*, 4630. (b) Norman, J. G., Jr. *Mol. Phys.* **1976**, *31*, 1198.

(45) In practice, the program calculates atomic radii for each atom and varies, as a percentage, the set to be used in the molecular potential. Limited computer time necessitates close but non-1 virial coefficients. For $\text{Co}(\text{CO})_3\text{L}_2'$, the converged virial coefficient equaled 0.99989.

(46) (a) Schwarz, K. *Phys. Rev. B* **1972**, *2466*. (b) Schwarz, K. *Theor. Chim. Acta* **1974**, *34*, 225.

(47) Slater, J. C. *Int. J. Quantum Chem.* **1973**, *7*, 533.

(48) Minimal basis set for $\text{Co}(\text{CO})_3\text{L}_2'$: Co, $l = 2$; C, $l = 1$; P, $l = 2$; H, $l = 0$.

The coordinates for $\text{Co}(\text{CO})_3\text{L}_2'$ were taken from the crystal structure of the related $\text{Co}(\text{CO})_3\text{L}_2$ complex in ref 23 and idealized to C_2 symmetry. The phenyl rings bonded to the P atoms in $\text{Co}(\text{CO})_3\text{L}_2$ were replaced by H atoms for the calculation. The coordinate system used is shown in Figure 2. The Co atom is placed at the origin, and the phosphorus, carbon, and oxygen atoms of the L_2' ligand lie in the yz plane. The axial CO ligand lies at an 11° angle from the x axis (in the positive y direction), and the two symmetry equivalent CO's are 34° below the yz plane. The coordination geometry around the cobalt atom is approximately square pyramidal. The mirror plane is the xy plane. Due to the unspherical nature of the molecule, the origin for the outer sphere was placed at the valence-electron-weighted average of all the other atom coordinates. The coordinates for all atoms, in bohrs, are found in the supplementary material.

Acknowledgment is made to the National Science Foundation for the support of this work. D.R.T. acknowledges the Alfred P. Sloan Foundation for a fellowship. Prof. P. C. Ford (UC Santa Barbara) is acknowledged for helpful discussions.

Supplementary Material Available: A table with the atom coordinates used in the calculation and a figure showing the linear relationship between the $\nu(\text{CO})$ frequencies and the band maximum of the lowest energy absorption band (2 pages). Ordering information is given on any current masthead page.

Alkyl-Transfer Reactions from Transition Metal Alkyl Complexes to $\text{CpFe}(\text{CO})_2^-$: Rate and Mechanistic Studies

Ping Wang and Jim D. Atwood*

Contribution from the Department of Chemistry, University at Buffalo, State University of New York, Buffalo, New York 14214. Received February 7, 1992

Abstract: We have examined reactions of several alkyl complexes ($\text{Mn}(\text{CO})_5\text{Me}$, $\text{Mn}(\text{CO})_5\text{CH}_2\text{Ph}$, $\text{Mn}(\text{CO})_5\text{Ph}$, $\text{CpMo}(\text{CO})_3\text{Me}$, $\text{CpMo}(\text{CO})_3\text{Et}$, and $\text{CpMo}(\text{CO})_3\text{CH}_2\text{Ph}$) with $\text{CpFe}(\text{CO})_2^-$. Each of these reactions results in transfer of the alkyl group to the iron with formation of $\text{Mn}(\text{CO})_5^-$ or $\text{CpMo}(\text{CO})_3^-$. The reactions were first order in the concentration of $\text{CpFe}(\text{CO})_2^-$ and first order in the alkyl complex. The dependence on the group transferred, $\text{H}^+ > \text{CH}_2\text{Ph}^+ > \text{Me}^+ > \text{Et}^+ > \text{Ph}^+$, is consistent with a nucleophilic attack mechanism. For methyl transfer the rate correlates with the difference in nucleophilicity between the reactant and product anions. We have also evaluated the self-exchange between $\text{CpFe}(\text{CO})_2\text{Me}$ and $\text{CpFe}(\text{CO})_2^-$ by line-broadening experiments. Our attempt to estimate the self-exchange rate constant for $\text{CpMo}(\text{CO})_3\text{Me}$ and $\text{CpMo}(\text{CO})_3^-$ shows this reaction to occur very slowly through a methyl migration sequence.

Electron transfer in organic and organometallic reactions is recognized as a crucial step in many important reactions.^{1,2} Atom-transfer reactions, while common for organic systems,³ are

(1) (a) Ebersson, L. *Electron Transfer Reactions in Organic Chemistry*; Springer-Verlag: Berlin, 1987 and references therein.

(2) (a) Wender, I.; Pino, P. *Metal Carbonyls in Organic Synthesis*; Wiley-Interscience: New York, 1968. (b) Ellis, J. E. *J. Organomet. Chem.* **1975**, *86*, 1. (c) Chini, P.; Longoni, G.; Albano, V. G. *Adv. Organomet. Chem.* **1976**, *14*, 285. (d) Hershberger, J. W.; Klingler, R. J.; Kochi, J. K. *J. Am. Chem. Soc.* **1982**, *104*, 3034. (e) Schmidt, S. P.; Basolo, F. *Inorg. Chim. Acta* **1987**, *131*, 181. (f) Connelly, N. G.; Dahl, L. F. *J. Chem. Soc., Chem. Commun.* **1970**, 880. (g) Braddock, J. N.; Meyer, T. J. *Inorg. Chem.* **1973**, *12*, 723. (h) Libson, K.; Woods, M.; Sullivan, J. C.; Watkins, J. W., II; Elder, R. C.; Deutsch, E. *Inorg. Chem.* **1988**, *27*, 999. (i) Protasiewicz, J. D.; Theopold, K. H.; Schulte, G. *Inorg. Chem.* **1988**, *27*, 1136. (j) Lee, K. Y.; Kochi, J. K. *Inorg. Chem.* **1989**, *28*, 567. (k) Lee, K. Y.; Kuchynka, D. J.; Kochi, J. K. *Organometallics* **1987**, *6*, 1886. (l) Kuchynka, D. J.; Amatore, C.; Kochi, J. K. *Inorg. Chem.* **1988**, *27*, 2574. (m) Kuchynka, D. J.; Kochi, J. K. *Inorg. Chem.* **1989**, *28*, 855. (n) Troglor, W. C., Ed. *Organometallic Radical Processes*; Elsevier: Amsterdam, 1990.

(3) McCortney, B. A.; Jacobson, B. M.; Vreeke, M.; Lewis, E. S. *J. Am. Chem. Soc.* **1990**, *112*, 3554 and references therein. (b) Berenius, P. *Acta Chem. Scand.* **1961**, *15*, 1151. (c) Ritchie, C. D.; Lu, S. *J. Am. Chem. Soc.* **1990**, *112*, 7748. (d) Parker, V. D.; Chao, Y.; Reitstoen, B. *J. Am. Chem. Soc.* **1991**, *113*, 2337. (e) McCortney, B. A.; Jacobsen, B. M.; Vreeke, M.; Lewis, E. S. *J. Am. Chem. Soc.* **1990**, *112*, 3554.

Table I. Carbonyl Stretching Frequencies of the Alkyl Complexes in Hexane

compound	ν_{CO} (cm^{-1})
$\text{Mn}(\text{CO})_5\text{Me}$	2110 (w), 2012 (s), 1991 (s)
$\text{Re}(\text{CO})_5\text{Me}$	2127 (w), 2041 (w), 2013 (s), 1983 (s)
$\text{CpFe}(\text{CO})_2\text{Me}$	2014 (s), 1960 (s)
$\text{CpMo}(\text{CO})_3\text{Me}$	2024 (s), 1941 (s)
$\text{CpMo}(\text{CO})_3\text{Et}$	2009 (s), 1935 (s)
$\text{Mn}(\text{CO})_5\text{CH}_2\text{Ph}$	2107 (s), 2043 (w), 2010 (s), 1992 (s)
$\text{CpMo}(\text{CO})_3\text{CH}_2\text{Ph}$	2019 (s), 1944 (sh), 1936 (s)
$\text{PhMn}(\text{CO})_5$	2115 (m), 2045 (w), 2020 (s), 1998 (s), 1985 (w)

less commonly observed for organometallic complexes. Hydrogen transfer, as a proton⁴ and as an atom,⁵ has been reported. The

(4) (a) Jordan, R. F.; Norton, J. R. *J. Am. Chem. Soc.* **1982**, *104*, 1255. (b) Weberg, R. T.; Norton, J. R. *J. Am. Chem. Soc.* **1990**, *112*, 1105. (c) Kristj nsd ttir, S. S.; Moody, A. E.; Weberg, R. T.; Norton, J. R. *Organometallics* **1988**, *7*, 1983. (d) Edidin, R. T.; Sullivan, J. M.; Norton, J. R. *J. Am. Chem. Soc.* **1987**, *109*, 3945. (e) Moore, E. J.; Sullivan, J. M.; Norton, J. R. *J. Am. Chem. Soc.* **1986**, *108*, 2257. (f) Kristj nsd ttir, S. S.; Norton, J. R. *J. Am. Chem. Soc.* **1991**, *113*, 4366. (g) Ryan, O. B.; Tilset, M.; Parker, V. D. *Organometallics* **1991**, *10*, 298. (h) Ryan, O. B.; Tilset, M.; Parker, V. D. *J. Am. Chem. Soc.* **1990**, *112*, 2618. (i) Miller, A. E. S.; Kawamura, A. R. *J. Am. Chem. Soc.* **1990**, *112*, 457.